Molecular Therapy
Methods & Clinical Development
Original Article

Gene therapy using human FMRP isoforms driven by the human *FMR1* promoter rescues fragile X syndrome mouse deficits

Yiru Jiang,[1,2,5] Linkun Han,[1,5] Jian Meng,[1] Zijie Wang,[1] Yunqiang Zhou,[1] Huilong Yuan,[1] Hui Xu,[1] Xian Zhang,[1] Yingjun Zhao,[1] Jinsheng Lu,[2,3] Huaxi Xu,[1] Chen Zhang,[4] and Yun-wu Zhang[1]

[1]Xiamen Key Laboratory of Brain Center, The First Affiliated Hospital of Xiamen University, and Fujian Provincial Key Laboratory of Neurodegenerative Disease and Aging Research, Institute of Neuroscience, School of Medicine, Xiamen University, Xiamen, Fujian 361102, China; [2]Emergency Department, Xiang'an Hospital of Xiamen University, Xiamen, Fujian 361102, China; [3]Geriatrics Department, Geriatric Hospital of Hainan, Haikou, Hainan 571100, China; [4]School of Basic Medical Sciences, Beijing Key Laboratory of Neural Regeneration and Repair, Capital Medical University, Beijing 100069, China

Fragile X syndrome (FXS) is caused by the loss of the fragile X messenger ribonucleoprotein 1 (FMRP) encoded by the *FMR1* gene. Gene therapy using adeno-associated virus (AAV) to restore FMRP expression is a promising therapeutic strategy. However, so far AAV gene therapy tests for FXS only utilized rodent FMRPs driven by promoters other than the human *FMR1* promoter. Restoration of human FMRP in appropriate cell types and at physiological levels, preferably driven by the human *FMR1* promoter, would be more suitable for its clinical use. Herein, we generated two human *FMR1* promoter subdomains that effectively drive gene expression. When AAVs expressing two different human FMRP isoforms under the control of a human *FMR1* promoter subdomain were administered into bilateral ventricles of neonatal *Fmr1*$^{-/y}$ and wild-type (WT) mice, both human FMRP isoforms were expressed throughout the brain in a pattern reminiscent to that of mouse FMRP. Importantly, human FMRP expression attenuated social behavior deficits and stereotyped and repetitive behavior, and reversed dysmorphological dendritic spines in *Fmr1*$^{-/y}$ mice, without affecting WT mouse behaviors. Our results demonstrate that human *FMR1* promoter can effectively drive human FMRP expression in the brain to attenuate *Fmr1*$^{-/y}$ mouse deficits, strengthening the notion of using AAV gene therapy for FXS treatment.

INTRODUCTION

Fragile X syndrome (FXS) is a neurodevelopmental disorder caused by mutations in the X-linked *FMR1* gene. The 5′ untranslated region of the *FMR1* gene contains a CGG-triplet repeat that may subject to unstable expansion. Healthy people carry less than 55 CGG repeats. Excessive CGG expansion can cause abnormal methylation and thus lead to partial (55–200 CGG repeats) or complete (>200 CGG repeats) abolishment of production of the *FMR1*-encoded protein, fragile X messenger ribonucleoprotein 1 (FMRP). FMRP is an RNA-binding protein and regulates numerous mRNAs important for synapse maturation and function. Thereby, loss of FMRP can result in FXS with clinical manifestations of intellectual disability and autism spectrum disorder (ASD)-related behaviors.[1-3]

The *FMR1* gene is subjected to complicated alternative splicing that affects the presence of exons 12 and 14, as well as the choice of acceptor sites in exons 15 and 17. Multiple *FMR1*/*Fmr1* mRNA and FMRP protein isoforms have been found to be expressed in human and rodent cells and tissues.[4-9] Interestingly, different FMRP isoforms have different subcellular localizations, implicating that these FMRP isoforms may have independent functions and their loss may lead to FXS through multiple pathophysiological pathways.[4,10]

Currently there is no cure for FXS. Pharmacotherapeutic approaches, such as stimulants, antidepressants, and antipsychotics, are used for symptom treatment of comorbid behaviors and psychiatric problems, but do not target the underlying cause of FXS.[1-3] As a single-gene disorder, viral vector-based gene therapy using adeno-associated virus (AAV) vectors provides a promising strategy for FXS treatment.[3,11] Several studies have explored the potential of using AAV-mediated FMRP expression for FXS treatment in animal models. Overall, these studies demonstrate that restoration of FMRP at least partially reversed altered biochemical and physiological features and attenuated behavioral deficits in rodent FXS models.[2,12-15] However, all these studies used rodent FMRP and the expression was driven by promoters other than the human *FMR1* promoter. To apply AAV gene therapy for FXS clinical tests in the future, the therapeutic efficacy of human FMRP expression in appropriate cells and at physiological levels, preferably driven by the human *FMR1* gene promoter

Received 20 April 2022; accepted 4 October 2022;
https://doi.org/10.1016/j.omtm.2022.10.002.

[5]These authors contributed equally

Correspondence: Yun-wu Zhang, Xiamen Key Laboratory of Brain Center, The First Affiliated Hospital of Xiamen University, and Xiamen Fujian Provincial Key Laboratory of Neurodegenerative Disease and Aging Research, Institute of Neuroscience, School of Medicine, Xiamen University, Xiamen, Fujian 361102, China.
E-mail: yunzhang@xmu.edu.cn

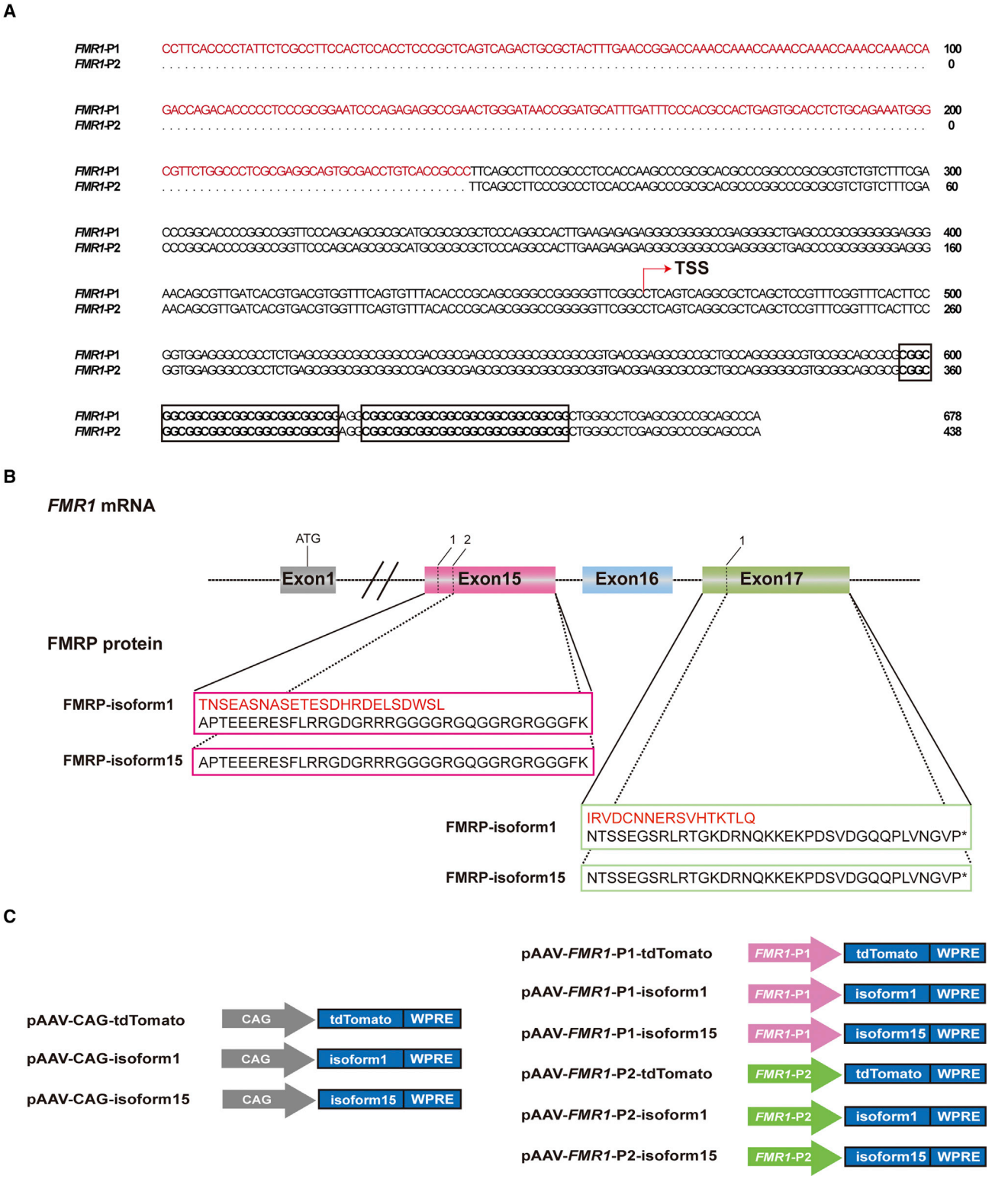

(legend on next page)

should be determined. Moreover, it was recently found that diacylglycerol kinase kappa (DGKk) levels were decreased in the brain of *Fmr1*$^{-/y}$ mice and that AAV-mediated expression of DGKk attenuated abnormal cerebral diacylglycerol/phosphatidic acid homeostasis and FXS-relevant behavioral phenotypes in *Fmr1*$^{-/y}$ mice,[16] suggesting that an alternative gene therapy approach is also beneficial for FXS treatment.

In this study, we generated AAV2/9s that express two different human FMRP isoforms driven by a human *FMR1* promoter subdomain, and injected them into lateral ventricles of postnatal day 0 (P0) male *Fmr1* knockout (KO) (*Fmr1*$^{-/y}$) mice and wild-type (WT) male mice. We found that the human *FMR1* promoter subdomain effectively drove gene expression in neurons in multiple mouse brain regions. Exogenous expression of the two human FMRP isoforms had no effect on the cognitive memory and social behavior in WT mice. Importantly, expression of both human FMRPs alleviated the social behavior deficits and stereotyped and repetitive behavior, and reversed the impaired dendritic spine morphologies in *Fmr1*$^{-/y}$ mice.

RESULTS

Generation of AAVs that have different human FMRP isoform expressions driven by a human *FMR1* promoter subdomain

A previous study identified a nearly 660-bp deletion of the 5′ region of the *FMR1* gene in a patient with intellectual disability. This deleted fragment includes the CpG island, the transcription initiation site, and the CGG triplet repeat; and its deletion abolished the transcription of *FMR1*.[17] Therefore, we believe that this fragment contains the core promoter region of *FMR1* and synthesized this sequence to replace the CAG promoter for driving gene expression in the AAV system. The exact *FMR1* promoter subdomain sequence we synthesized is 678 bp long (*FMR1*-P1, Figure 1A), with several CGG triplets more than the published sequence.[17] We also used a truncated *FMR1* promoter subdomain (*FMR1*-P2, Figure 1A) that lacks the 240 bp of the 5′-end of *FMR1*-P1.

Human FMRP isoform 1 (isoform nomenclature follows that in Pretto et al.[9]) is the longest isoform (632 amino acids) and its mouse counterpart is the most widely used isoform in AAV therapeutic studies. Interestingly, through direct PCR amplification (Figure S1) and sequencing we identified FMRP isoform 15 in cDNAs of human HEK293T cells, one of the most used cell lines in biological research, as well as of human neuroblastoma SH-SY5Y cells. These results suggest that FMRP isoform 15 mRNA is an abundantly expressed isoform, although FMRP isoform 15 protein expression was minimal in HEK293T cells (Figure 2C) for unknown reasons. Human FMRP isoform 15 transcript uses the second different acceptor site at exon 15 and a different acceptor site at exon 17; and human FMRP isoform 15 lacks amino acids 491–515 and 580–596 compared with human FMRP isoform 1 (Figure 1B). In this study, we investigated therapeutic values of both FMRP isoform 1 and isoform 15. The AAV plasmids constructed and used are shown in Figure 1C.

To determine whether the two synthesized human *FMR1* promoter subdomains can effectively drive gene expression, we transfected HEK293T cells with various plasmids. Western blotting results showed that both *FMR1*-P1 (Figures 2A and 2B) and *FMR1*-P2 (Figures 2C and 2D) effectively drove the expression of FMRP isoform 1 and isoform 15, although their promoter activities were weaker than that of the CAG promoter (Figures 2A–2D). Between the two *FMR1* promoter subdomains, *FMR1*-P2 had significantly stronger promoter activity than *FMR1*-P1 (Figures 2A–2D).

Next, we used AAV plasmids containing the *FMR1*-P2 promoter for virus packaging (serotype 2/9). AAV2/9s were then administered into the brain of neonatal *Fmr1*$^{-/y}$ and WT male mice through intracerebroventricular (i.c.v.) injection. Animal behaviors were tested at age 1.5 months and mice were sacrificed at about age 2–3 months for biochemical studies (Figure 3A). Immunofluorescence analysis showed that the *FMR1*-P2 promoter drove tdTomato expression throughout the brain in WT mice, with strong expression in the cerebral cortex and hippocampus (Figure S2A). *FMR1*-P2 also drove exogenous human FMRP isoform 1 and isoform 15 expression widely in the brain of *Fmr1*$^{-/y}$ mice, in a distribution pattern similar to that of endogenous mouse FMRP (Figures 3B and S3). Exogenous human FMRP isoform 1 and isoform 15, as well as endogenous mouse FMRP in WT mice expressing the two human FMRP isoforms at about age 2.5 months, dominantly colocalized with the neuronal marker NeuN but not with the astrocytic marker GFAP (Figure S2B), indicating that these FMRPs are mainly expressed in neurons at adult age and this is consistent with previous findings.[18] Moreover, the subcellular localizations of human FMRP isoform 1 and isoform 15 were in the cytosol, consistent with the subcellular localization of endogenous mouse FMRP (Figure 3C).

Endogenous mouse FMRP were found to be expressed in multiple isoforms in the three major neural cell types: neurons, astrocytes, and microglia (Figure 3D). We found that the molecular size of human FMRP isoform 1 was similar to those of the major FMRP isoforms in mouse primary neurons and astrocytes, whereas the molecular size of human FMRP isoform 15 was similar to that of the major FMRP isoform in mouse primary microglia (Figure 3D). We also determined that the expression levels of human FMRP isoform 1 and isoform 15 in *Fmr1*$^{-/y}$ mice were about 75% and 73% of the

Figure 1. Schemes of human *FMR1* promoters, human FMRP isoforms, and AAV vectors used in this study

(A) Sequence alignment of the two human promoter subdomains *FMR1*-P1 and *FMR1*-P2. Sequence differences between them are in red. The transcription start site (TSS) is indicated by an arrow. The CGG repeats are highlighted in squared frames. (B) Schematic differences between human FMRP isoform 1 and isoform 15. The transcript of human FMRP isoform 15 uses the second different acceptor site on *FMR1* exon 15 and a different acceptor site on *FMR1* exon 17. Human FMRP isoform 15 lacks amino acids 491–515 and 580–596 compared with human FMRP isoform 1. These missing amino acids are highlighted in red. ATG, translation start codon. (C) AAV vectors used in this study, including vectors expressing tdTomato, human FMRP isoform 1, and human FMRP isoform 15 that are driven by CAG, *FMR1*-P1, and *FMR1*-P2.

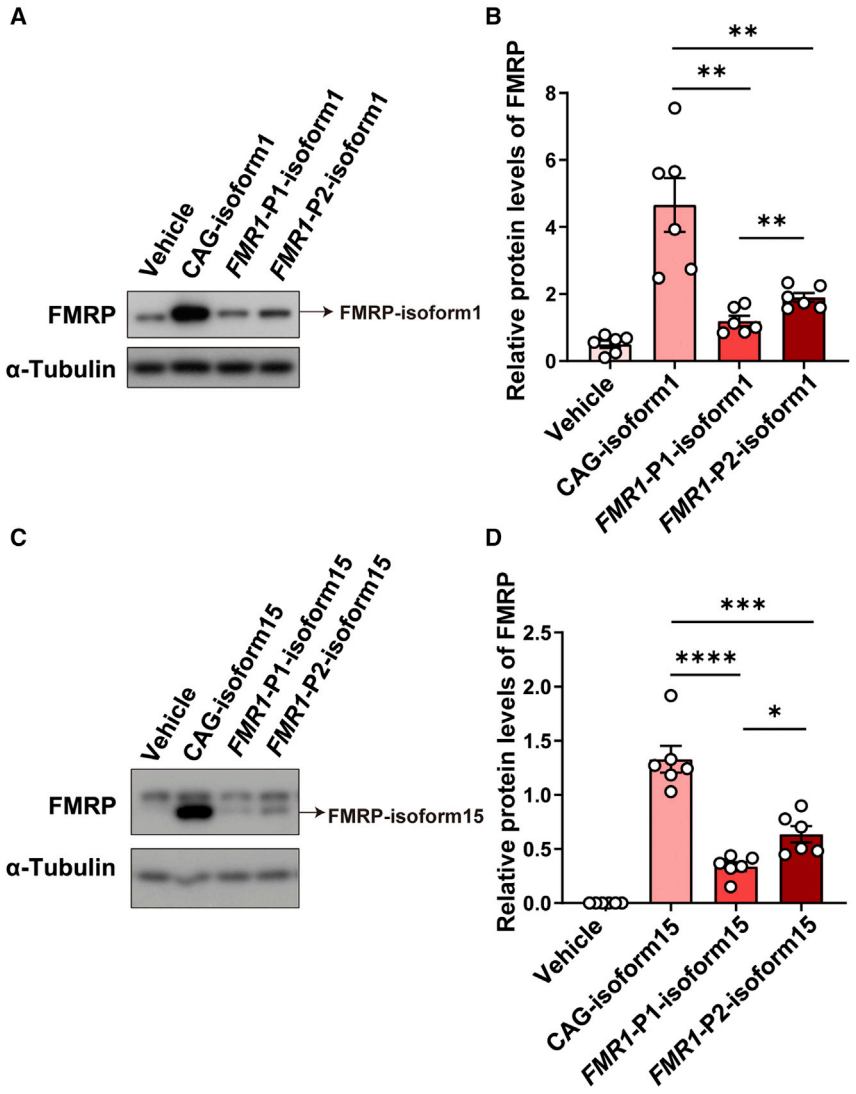

Figure 2. Comparison of the activity of the two *FMR1* promoter subdomains

(A and B) Plasmids expressing human FMRP isoform 1 driven by CAG, *FMR1*-P1, and *FMR1*-P2 promoter subdomains, as well as the AAV-CAG-tdTomato plasmid (as vehicle control) were transiently transfected into HEK293T cells. Equal amounts of protein lysates were assayed by western blot (A), and FMRP protein levels were quantified by densitometry and normalized to those of α-tubulin for comparison (B). (C and D) Plasmids expressing human FMRP isoform 15 driven by CAG, *FMR1*-P1, and *FMR1*-P2 promoter subdomains, as well as the AAV-CAG-tdTomato plasmid (as vehicle control) were transiently transfected into HEK293T cells. Equal amounts of protein lysates were assayed by western blot (C), and FMRP protein levels were quantified by densitometry and normalized to those of α-tubulin for comparison (D). Data are presented as the mean ± SEM. One-way ANOVA test was used. n = 6 per group. *p < 0.05, **p < 0.01, ***p < 0.001, ****p < 0.0001.

endogenous total FMRP levels in WT mice, respectively (Figures 3E and 3F), and the overall FMRP expression levels in WT mice expressing human FMRP isoform 1 and isoform 15 were about 161% and 175% of those in control mice, respectively (Figures S2C and S2D).

Expression of human FMRP does not affect locomotor activity, memory, and social activity in WT mice

We injected different AAV2/9s into P0 C57BL/6J mice to study whether exogenous expression of human FMRP could adversely affect WT mice (Figure 4A). In the open-field test, there were no differences in the time spent in the central area and the total distance traveled between WT mice administered with control AAVs and with AAVs expressing human FMRP isoform 1 or isoform 15 (Figures 4B and 4C). In the elevated plus-maze test, there were also no differences in the exploration time in the open arms among the three groups of mice (Figure 4D), suggesting that exogenous expression of the two human FMRP isoforms has no effect on mouse locomotor activity and anxiety. In the Y-maze test, all three groups of mice showed no differences in their spontaneous alternations (Figure 4E). In the novel object recognition test, the three groups of mice spent significantly more time exploring the novel object than the familiar object and there were no differences among them (Figure 4F). These results suggest that exogenous expression of the two human FMRP isoforms has no effect on mouse short-term working memory and recognition memory. In the three-chamber social interaction test, mice with exogenous expression of the two human FMRP isoforms exhibited similar social preference (Figure 4G) and social novelty recognition (Figure 4H) to those of control mice. In the nest building test, there were no significant differences in nesting scores among the three groups of mice (Figure 4I). In the self-grooming test, there were also no significant differences in the time spent grooming and the number of bouts among the three groups of mice (Figures 4J and 4K). These results indicate that exogenous expression of the two human FMRP isoforms does not affect social and stereotyped and repetitive behaviors in WT mice.

Expression of human FMRP does not affect locomotor activity and memory in *Fmr1*$^{-/y}$ mice

We then injected different AAV2/9s into P0 *Fmr1*$^{-/y}$ and their WT control mice in FVB background (Figure 5A). At age 1.5 months, we found that *Fmr1*$^{-/y}$ mice administered with AAV controls (*Fmr1*$^{-/y}$ + AAV-control) had comparable time spent in the central area and total travel distance in the open-field test when compared with WT mice administered with AAV controls (WT + AAV-control,

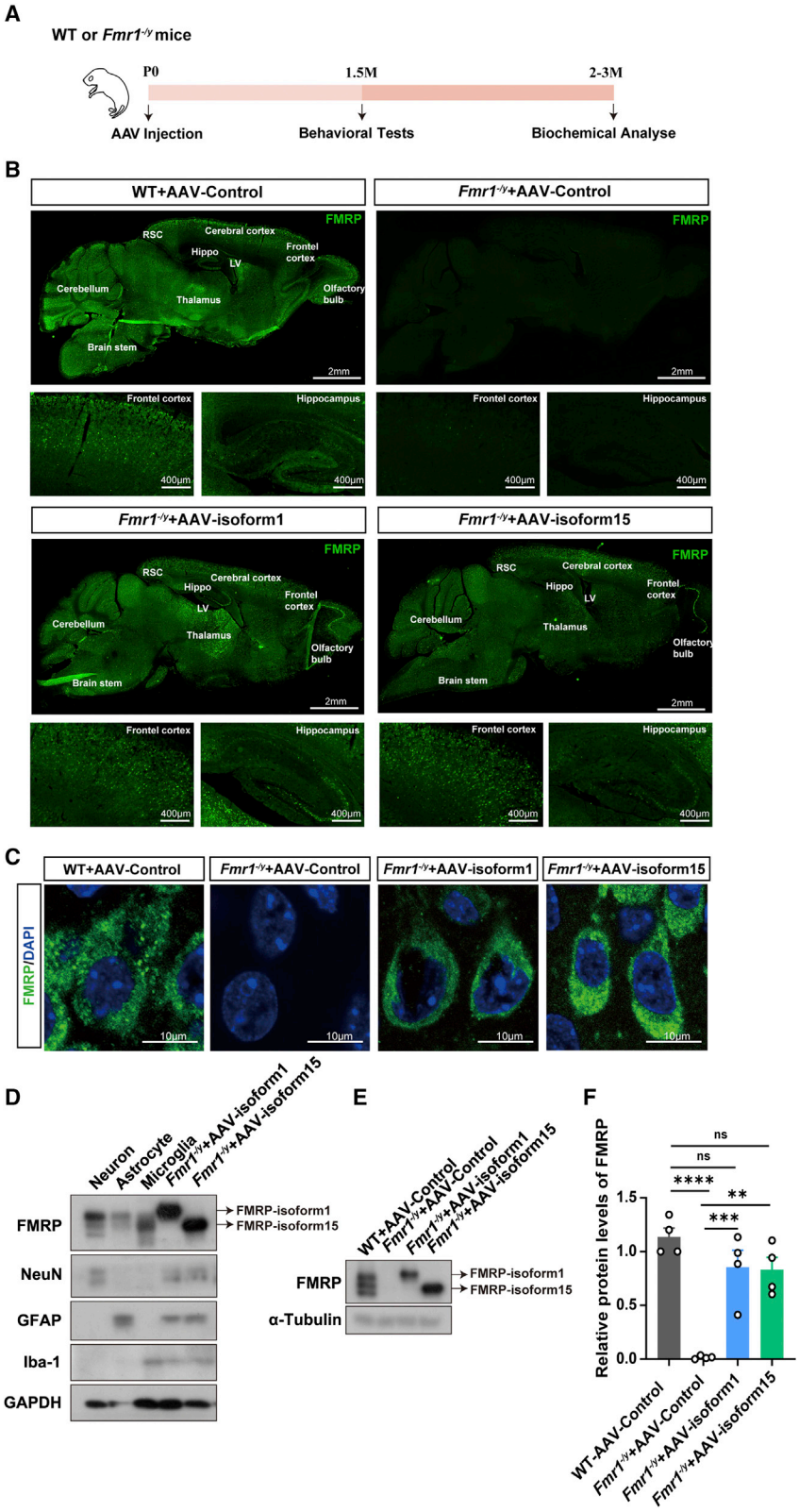

Figure 3. AAV-mediated FMRP expression in the mouse brain

(A) Experimental procedure scheme. AAVs were i.c.v. injected into the brain of postnatal day 0 (P0) mice. Behavioral tests were carried out at age 1.5 months. Mice were sacrificed at about age 2–3 months for biochemical studies. (B) P0 FVB WT mice were injected with AAV-*FMR1*-P2-tdTomato (WT + AAV-control) and *Fmr1*$^{-/y}$ mice were injected with AAV-*FMR1*-P2-tdTomato (*Fmr1*$^{-/y}$ + AAV-control), AAV-*FMR1*-P2-isoform 1 (*Fmr1*$^{-/y}$ + AAV-isoform 1), or AAV-*FMR1*-P2-isoform 15 (*Fmr1*$^{-/y}$ + AAV-isoform 15). At age 2.5 months, mouse brains were collected and sectioned sagittally for immunostaining of FMRP (in green). The nuclei were stained by DAPI (in blue). Scale bars, 2 mm (for full images) and 400 μm (for enlarged images). RSC, retrosplenial granular cortex; LV, lateral ventricle; Hippo, hippocampus. (C) Magnification of cells in the CA3 regions in (B). Scale bars, 10 μm. (D) Equal amounts of protein lysates from mouse primary neurons, astrocytes, and microglia, and from hippocampus of *Fmr1*$^{-/y}$ + AAV-isoform 1 and *Fmr1*$^{-/y}$ + AAV-isoform 15 mice were subjected to western blot for FMRP, NeuN (neuronal marker), GFAP (astrocytic marker), Iba1 (microglial marker), and GAPDH (as control). (E) Equal amounts of protein lysates from hippocampus of WT + AAV-control, *Fmr1*$^{-/y}$ + AAV-control, *Fmr1*$^{-/y}$ + AAV-isoform 1, and *Fmr1*$^{-/y}$ + AAV-isoform 15 mice were subjected to western blot. (F) FMRP levels were quantified and normalized to those of α-tubulin for comparison. Data are presented as the mean ± SEM. One-way ANOVA was used. n = 4 per group. $^{**}p < 0.01$, $^{***}p < 0.001$, $^{****}p < 0.0001$; ns, not significant.

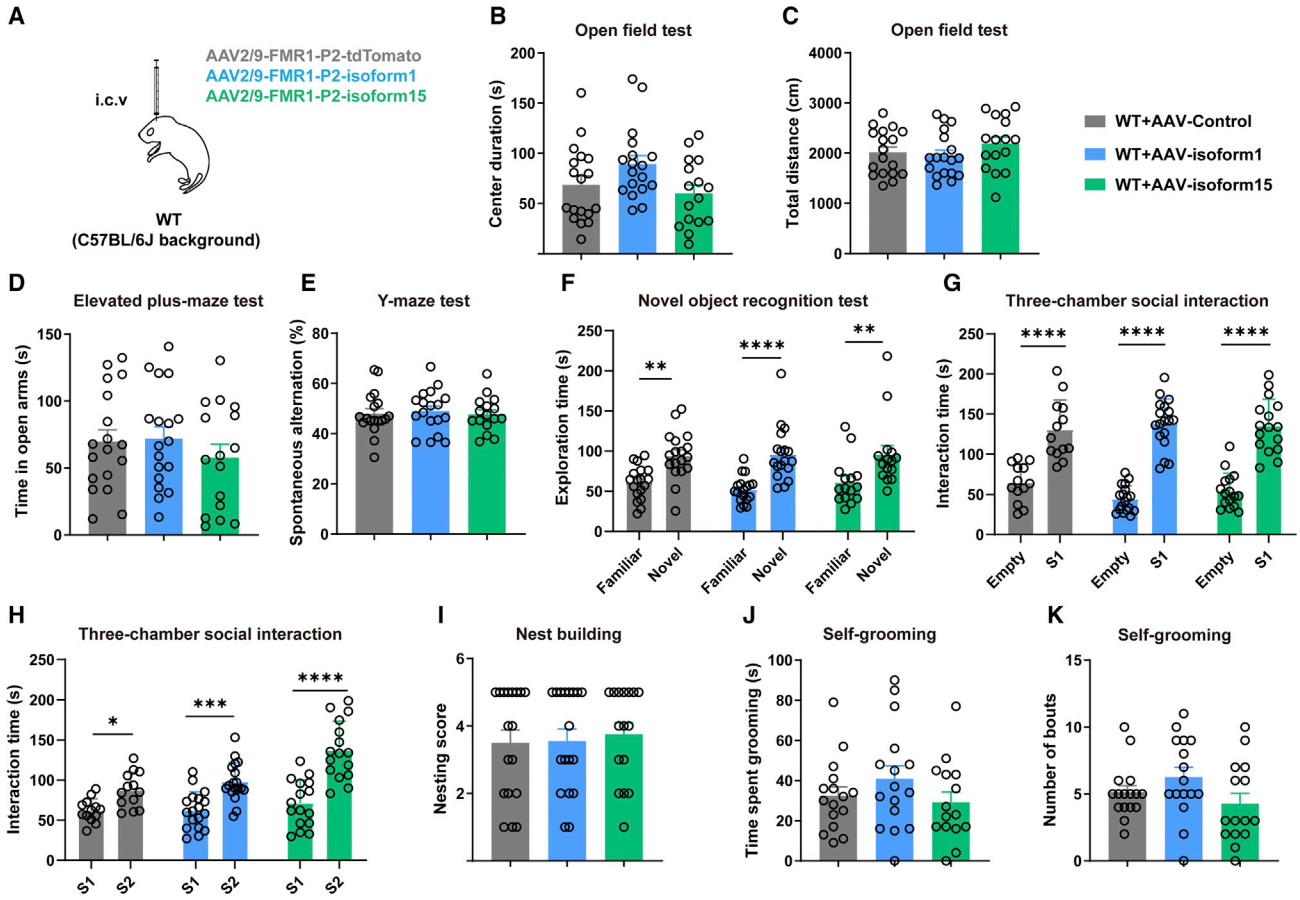

Figure 4. Expression of human FMRPs does not affect locomotor activity, memory, and social activity in WT mice

(A) Neonatal C57BL/6J WT mice were injected with AAV-*FMR1*-P2-tdTomato (WT + AAV-control), AAV-*FMR1*-P2-isoform 1 (WT + AAV-isoform 1), or AAV-*FMR1*-P2-isoform 15 (WT + AAV-isoform 15). (B and C) In the open-field test, time spent in the central area (B) and the total travel distance (C) were studied. (D) In the elevated plus-maze test, the times in the open arm were studied. (E) In the Y-maze test, the percentages of spontaneous alternation within the three arms were studied. (F) In the novel object recognition test, the times of mice to explore the novel object and the familiar object were recorded for comparison. (G and H) In the three-camber social interaction test, the time spent interacting with an empty cage or a strange mouse (S1) was measured to evaluate social preference (G), and the time spent interacting with S1 or another strange mouse (S2) was measured to evaluate social novelty (H). (I) In the nest building test, the nest building scores were measured for comparison. (J and K) In the self-grooming test, the time spent grooming (J) and bout numbers (K) were studied. Data are presented as the mean ± SEM. One-way ANOVA was used. WT + AAV-control, n = 18 (n = 13 for the three-chamber social interaction test, and n = 16 for the self-grooming and nest building tests); WT + AAV-isoform 1, n = 18 (n = 16 for the self-grooming test); WT + AAV-isoform 15, n = 16 (n = 15 for the self-grooming test). *p < 0.05, **p < 0.01, ***p < 0.001, ****p < 0.0001.

Figures 5B and 5C). Furthermore, *Fmr1*$^{-/y}$ + AAV-control mice showed no differences in their spontaneous alternations in the Y-maze test when compared with WT + AAV-control mice (Figure 5D), and had significantly more time exploring the novel object than the familiar object in a pattern similar to that of WT + AAV-control mice (Figure 5E). These results suggest that *Fmr1*$^{-/y}$ mice have normal locomotor activity and memory at this age. Moreover, we found that *Fmr1*$^{-/y}$ mice administered with human FMRP isoform 1 (*Fmr1*$^{-/y}$ + AAV-isoform 1) and with isoform 15 (*Fmr1*$^{-/y}$ + AAV-isoform 15) exhibited comparable activities with those of *Fmr1*$^{-/y}$ + AAV-control mice in all these behavioral tests (Figures 5B–5E), suggesting that neither exogenous expression of the two human FMRP isoforms affect locomotor activity and memory in *Fmr1*$^{-/y}$ mice at this age.

Expression of human FMRP reverses anxiety- and ASD-like behaviors in *Fmr1*$^{-/y}$ mice

Although there were no differences in the time spent in the central area between *Fmr1*$^{-/y}$ + AAV-control mice and WT + AAV-control mice in the open-field test, *Fmr1*$^{-/y}$ + AAV-control mice spent significantly less time than WT + AAV-control mice in the open arms in the elevated plus-maze test (Figure 6A), which has better sensitivity in determining anxiety-like behaviors than the open-field test. While *Fmr1*$^{-/y}$ + AAV-isoform 1 mice but not *Fmr1*$^{-/y}$ + AAV-isoform 15 mice had significantly increased time spent in the open arms compared with *Fmr1*$^{-/y}$ + AAV-control mice (Figure 6A). These results suggest that loss of *Fmr1* leads to anxiety-like behaviors in mice, whereas expression of human FMRP isoform 1 can reverse this phenotype.

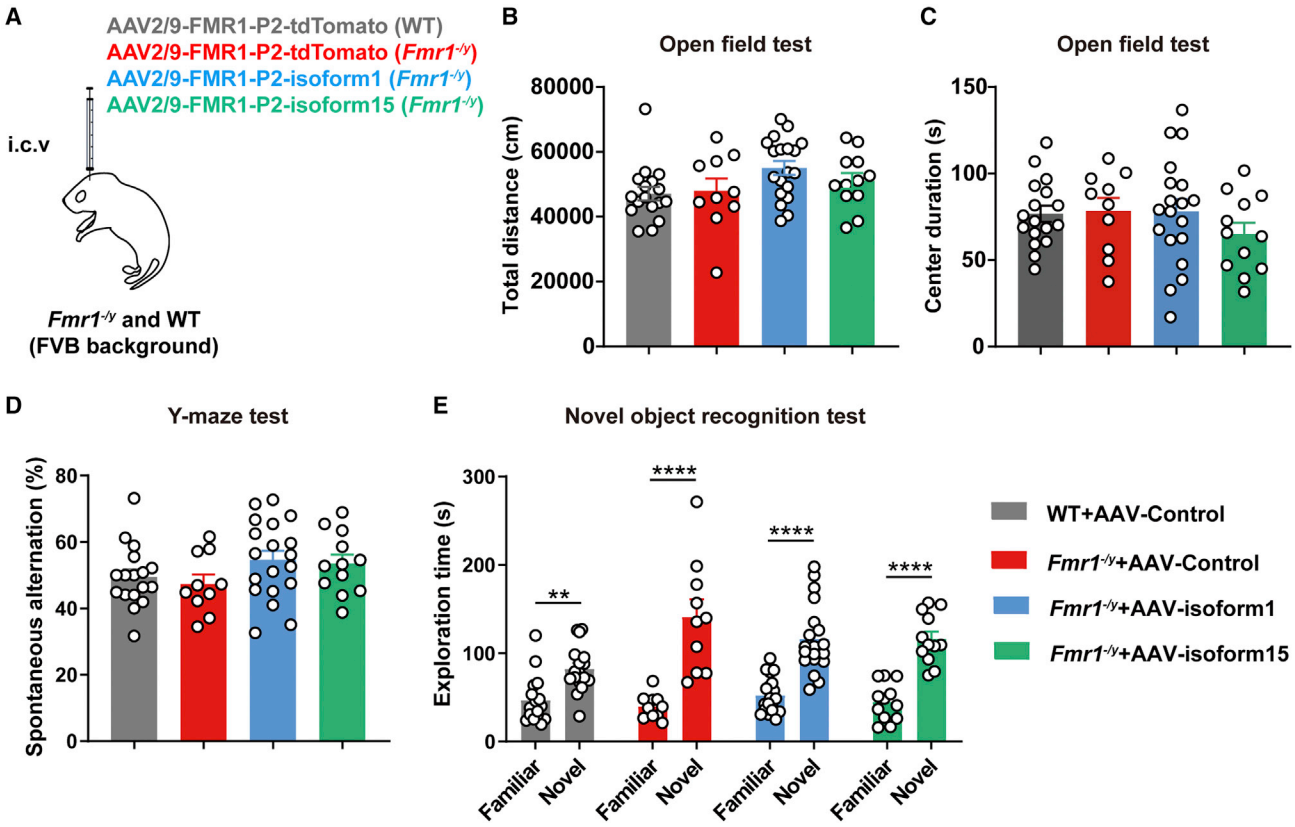

Figure 5. Expression of human FMRPs has no effect on locomotor activity and memory in *Fmr1*$^{-/y}$ mice

(A) Neonatal FVB WT mice were injected with AAV-*FMR1*-P2-tdTomato (WT + AAV-control, n = 17) and *Fmr1*$^{-/y}$ mice were injected with AAV-*FMR1*-P2-tdTomato (*Fmr1*$^{-/y}$ + AAV-control, n = 10), AAV-*FMR1*-P2-isoform 1 (*Fmr1*$^{-/y}$ + AAV-isoform 1, n = 19), or AAV-*FMR1*-P2-isoform 15 (*Fmr1*$^{-/y}$ + AAV-isoform 15, n = 12). (B and C) In the open-field test, the time spent in the central area (B) and total travel distance (C) were studied. (D) In the Y-maze test, the percentages of spontaneous alternation within the three arms were studied. (E) In the novel object recognition test, the time of mice explored the novel object and the familiar object were recorded for comparison. Data are presented as the mean ± SEM. One-way ANOVA was used. **p < 0.01, ****p < 0.0001.

In the three-chamber social interaction test, although all four groups of mice spent significantly more time exploring the cage with a strange mouse (S1) than with the empty cage when tested for their sociability (Figure 6B), *Fmr1*$^{-/y}$ + AAV-control mice showed no preference for another strange mouse (S2) over the familiar mouse S1 when tested for their social novelty, whereas WT + AAV-control mice, *Fmr1*$^{-/y}$ + AAV-isoform 1 mice, and *Fmr1*$^{-/y}$ + AAV-isoform 15 mice exhibited more preference for S2 than S1 (Figure 6C). In the nest building test, the nesting scores of *Fmr1*$^{-/y}$ + AAV-control mice were significantly lower than those of WT + AAV-control mice, whereas the nesting scores of *Fmr1*$^{-/y}$ + AAV-isoform 1 mice but not *Fmr1*$^{-/y}$ + AAV-isoform 15 mice were significantly higher than those of *Fmr1*$^{-/y}$ + AAV-control mice (Figure 6D). In the self-grooming test, *Fmr1*$^{-/y}$ + AAV-control mice exhibited significantly higher numbers of bout and time spent grooming when compared with WT + AAV-control mice, and expression of both human FMRP isoform 1 and isoform 15 significantly reduced the time spent grooming and bout numbers in *Fmr1*$^{-/y}$ mice (Figures 6E and 6F). Together, these results indicate that *Fmr1*$^{-/y}$ mice develop marked ASD-like behaviors, including social deficits and stereotyped and repetitive behavior, which can be attenuated by expression of the two human FMRP isoforms, especially isoform 1.

Expression of human FMRP alleviates dendritic spine abnormality in *Fmr1*$^{-/y}$ mice

Abnormal development of dendritic spines is one of the features and causal factors of FXS.[19-21] We further detected the changes of dendritic spines in mice by Golgi staining. The results showed that the numbers of mature dendritic spines in neurons in the layer V of cortex and hippocampus of *Fmr1*$^{-/y}$ mice were significantly decreased (Figures 7A and 7B), whereas the numbers of immature dendritic spines were significantly increased (Figures 7A and 7C) when compared with those of WT mice. Moreover, expression of both human FMRP isoform 1 and isoform 15 significantly reversed the decreased mature dendritic spine numbers and the increased immature dendritic spine numbers in *Fmr1*$^{-/y}$ mice (Figures 7A–7C).

DISCUSSION

AAV gene therapy has been successfully applied to treat genetic disorders, such as spinal muscular atrophy and RPE65 mutation-associated

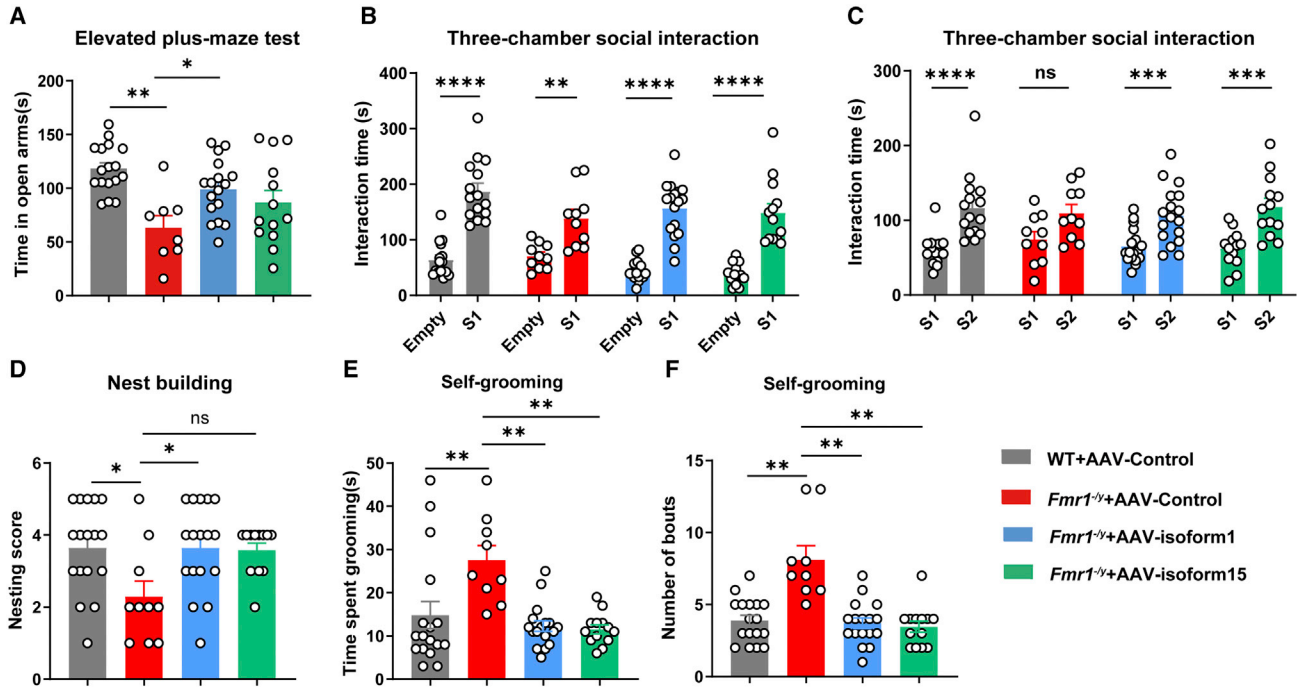

Figure 6. Expression of human FMRPs attenuates anxiety and ASD-like behaviors in *Fmr1*$^{-/y}$ mice

(A–F) Neonatal FVB WT mice were injected with AAV-*FMR1*-P2-tdTomato (WT + AAV-control) and *Fmr1*$^{-/y}$ mice were injected with AAV-*FMR1*-P2-tdTomato (*Fmr1*$^{-/y}$ + AAV-control), AAV-*FMR1*-P2-isoform 1 (*Fmr1*$^{-/y}$ + AAV-isoform 1), or AAV-*FMR1*-P2-isoform 15 (*Fmr1*$^{-/y}$ + AAV-isoform 15). In the elevated plus maze-test, the time in the open arm were compared (A). In three-chamber social interaction test, the time spent interacting with an empty cage or a strange mouse (S1) was measured to evaluate social preference (B), and the time spent interacting with S1 or another strange mouse (S2) was measured to evaluate social novelty (C). In the nest building test, the nest building scores were measured for comparison (D). In the self-grooming test, the time spent grooming (E) and bout numbers (F) were studied. Data are presented as the mean ± SEM. One-way ANOVA was used. WT + AAV-control, n = 17 (n = 15 for the three-chamber social interaction test); *Fmr1*$^{-/y}$ + AAV-control, n = 10 (n = 8 for the elevated plus-maze test, and n = 9 for the self-grooming test); *Fmr1*$^{-/y}$ + AAV-isoform 1, n = 17; *Fmr1*$^{-/y}$ + AAV-isoform 15, n = 13 (n = 12 for the nest building test). *p < 0.05, **p < 0.01, ***p < 0.001, ****p < 0.0001; ns, not significant.

retinal dystrophy. FXS is a single-gene disorder caused by the loss of FMRP function. Therefore, restoring FMRP by AAV gene therapy is promising for FXS therapeutics.[3,11] Zeier et al. first used a chicken β-actin core promoter with the cytomegalovirus immediate-early enhancer elements to drive the expression of murine FMRP isoform 1 tagged with an FLAG epitope.[13] They packaged AAVs with serotype 5 and injected AAVs into the hippocampus of *Fmr1* KO mice at 5 weeks of age. Three weeks later, they found that FMRP re-expression rescued abnormally enhanced long-term depression in *Fmr1* KO mice, implying that FMRP restoration may have the potential to improve cognitive function in FXS.[13] Gholizadeh et al. then used a human synapsin-1 promoter to drive murine FMRP isoform 1 expression and packaged AAVs with serotype 9.[12] They delivered AAVs into P5 *Fmr1* KO mice through bilateral i.c.v. injection, and analyzed behaviors at 22–26 and 50–56 days post injection. Their results showed that elevated repetitive behavior and social dominance behavior deficits were reversed upon FMRP re-expression, providing the first proof of principle that AAV gene therapy can correct behavioral abnormalities in the FXS mouse model.[12] The same group later also used serotype 9 AAVs expressing murine FMRP isoform 1 driven by the synapsin-1 promoter or a synapsin-1/CMV chimeric promoter and administered them into the brain of P0–P2 mice through bilateral i.c.v. injection.[14] They found that, at age 2–3 months, moderate FMRP re-expression at about 35%–115% of WT expression attenuated abnormal motor activity, anxiety, acoustic startle responses, and PSD-95 and MeCP2 expression in *Fmr1* KO mice.[14] Very recently, Yang et al. found that injecting serotype 9 AAVs into P0 and P35 mice to re-express murine FMRP isoform 1 (driven by the CMV promoter) ameliorated visual hypersensitivity in *Fmr1* KO mice.[15]

All the above studies used murine FMRP isoform 1. Since both human *FMR1* and murine *Fmr1* subject to complicated alternative splicing and FMRP isoforms have different subcellular localizations and thus potentially different functions,[4-10] it would be interesting to determine whether other FMRP isoforms also have therapeutic effect. Recently, Hooper et al. used rodent orthologs of another human FMRP isoform (numbered isoform 17 in Pretto et al.[9]) for gene therapy in *Fmr1* KO rats.[2] This *FMR1* isoform transcript lacks exon 12 and uses a different acceptor site at exon 17 compared with the longest *FMR1* isoform 1 transcript, therefore human FMRP isoform 17 lacks amino acids 376–396 and 580–596 compared with human FMRP isoform 1. Hooper et al. injected serotype 9 AAVs expressing

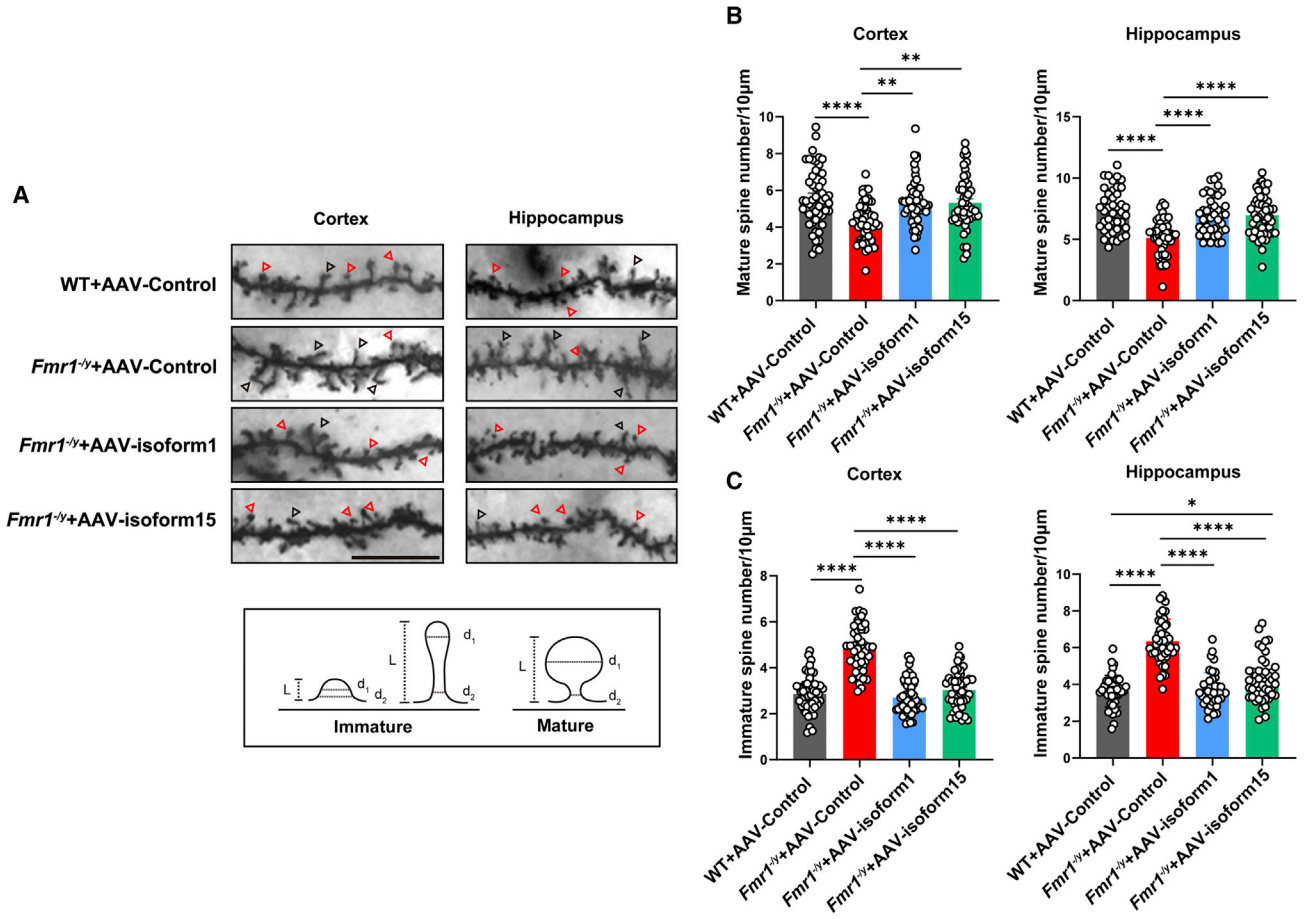

Figure 7. Expression of human FMRPs alleviates dendritic spine abnormality in *Fmr1*$^{-/y}$ mice

(A–C) Neonatal FVB WT mice were injected with AAV-*FMR1*-P2-tdTomato (WT + AAV-control) and *Fmr1*$^{-/y}$ mice were injected with AAV-*FMR1*-P2-tdTomato (*Fmr1*$^{-/y}$ + AAV-control), AAV-*FMR1*-P2-isoform 1 (*Fmr1*$^{-/y}$ + AAV-isoform 1), or AAV-*FMR1*-P2-isoform 15 (*Fmr1*$^{-/y}$ + AAV-isoform 15). Mouse brains were collected and sectioned for Golgi staining to show mature (indicated by red triangles) and immature (indicated by black triangles) dendritic spines in the layer V of cortex and the hippocampus (A). Scale bar, 10 μm. The numbers of mature (B) and immature (C) dendritic spines in the cortex and hippocampus of the four groups of mice were counted for comparison. Data are presented as the mean ± SEM. One-way ANOVA was used. n = 40 sections from three mice per group. *p < 0.05, **p < 0.01, ****p < 0.0001.

rodent orthologs of human FMRP isoform 17 driven by an MeCP2-mini promoter into the brain of P2–P3 rats through bilateral i.c.v. injection. They found that, at age 1.5–2 months, transgene expression partially rescued social dominance and locomotor activity deficits, and abnormal slow-wave activity during the sleep-like state in *Fmr1* KO rats.[2] Nevertheless, so far, all reported AAV gene therapy studies used rodent FMRP and the expression was driven by promoters other than the human *FMR1* promoter. To apply AAV gene therapy for FXS clinical tests in the future, the therapeutic efficacy of human FMRP expression in appropriate cell types and at physiological levels, preferably driven by the human *FMR1* gene promoter should be determined.

In this study, we investigated whether AAV gene therapy with expression of different human FMRP isoforms driven by the human *FMR1* promoter can rescue FXS-like phenotypes in *Fmr1* KO mice. We first compared two human *FMR1* promoter subdomains (*FMR1*-P1 and *FMR1*-P2) and found that both had reasonable promoter activity, although lower than that of the CAG promoter. Since *FMR1*-P2 had stronger promoter activity than *FMR1*-P1, we used *FMR1*-P2 for *in vivo* studies. When AAV2/9s were applied, we found that *FMR1*-P2 effectively drove both human FMRP isoforms' expression specifically in neurons throughout the mouse brain, in a distribution pattern reminiscent to that of endogenous mouse FMRP. The overall expression levels of human FMRP isoform 1 and isoform 15 in *Fmr1*$^{-/y}$ mice were about 75% and 73% of normal WT mouse FMRP levels, respectively. Importantly, we demonstrated that expression of the two human FMRP isoforms, especially isoform 1 attenuated anxiety-like behaviors and ASD-like social deficits and stereotyped and repetitive behavior, as well as distorted dendritic spine morphologies in *Fmr1*$^{-/y}$ mice. Previously it was found that, when *Fmr1* KO mice were crossed with transgenic mice expressing human *FMR1* cDNA (under the control of a CMV promoter) or a yeast artificial chromosome containing the entire human *FMR1* gene, their

audiogenic seizure susceptibility and abnormal behaviors were attenuated.[22,23] Therefore, our results as well as others demonstrate that human FMRP can compensate its mouse ortholog in mice. One limitation of our study is that we injected AAV2/9s at P0, a time not applicable for human when the blood-brain barrier is not yet closed. Application of these AAV2/9s in older mice to study their efficacy deserves further scrutiny.

Excessive FMRP may have deleterious consequences, as people carrying extra *FMR1* copies have intellectual disability and developmental problems.[24-26] Transgenic mice with massive expression of human FMRP (over 10-fold above WT mouse FMRP levels) were also found to have increased anxiety and reduced motor activity.[14,23] One study using a synapsin-1 promoter or a synapsin-1/CMV chimeric promoter to drive mouse FMRP expression found that moderate FMRP re-expression at about 35%–115% of WT expression had a protective effect in *Fmr1* KO mice. However, excessive re-expression of FMRP in *Fmr1* KO mice (about 2.5- to 6-fold over WT) led to pathological motor hyperactivity and startle response suppression; while moderate FMRP overexpression of up to 2-fold had little effect on animal behaviors in WT mice.[14] Herein, we found that combined FMRP (both human and mouse forms) levels in WT mice expressing human FMRP isoform 1 and isoform 15 were about 161% and 175%, respectively, of total endogenous FMRP levels in WT control mice. Moreover, expression of human FMRP isoform 1 and isoform 15 had no adverse effect on locomotor activity, memory, anxiety, and social behaviors in WT mice, reinforcing the safety of using human *FMR1* promoters and human FMRP for gene therapy.

Expression of human FMRP isoform 1 had more profound effects on attenuating anxiety-like behaviors in the elevated plus-maze test and stereotyped behavior in the nest building test than expression of human FMRP isoform 15 in *Fmr1*$^{-/y}$ mice. Compared with human FMRP isoform 1, human FMRP isoform 15 lacks amino acids 491–515 and 580–596. The 580–596 amino acid domain in human FMRP is involved in localizing FMRP to Cajal bodies in FMRP isoforms lacking exon 14.[2,10] Although our results showed that human FMRP isoform 15 was expressed in the cytosol just like human FMRP isoform 1 and mouse endogenous FMRP, human FMRP isoform 15 may have slightly different subcellular localization in the cytosol and thus different function than that of human FMRP isoform 1. Alternatively, the brain distribution pattern of human FMRP isoform 1 seems to be more reminiscent to that of endogenous mouse FMRP than human FMRP isoform 15. All these differences may affect the rescuing effects of the two human FMRP isoforms.

Although FXS patients have intellectual disability,[27] cognitive assays on *Fmr1* KO mice have generated mixed results, with some showing learning and memory deficiency and some showing no such deficits in these mice (reviewed in Kazdoba et al.[28]). Herein, we did not observe any deficit in short-term working memory and recognition memory in *Fmr1*$^{-/y}$ mice compared with WT controls. Expression of human FMRP isoform 1 and isoform 15 had no effect on short-term working memory and recognition memory in *Fmr1*$^{-/y}$ mice as well. Future work using better animal models may help determine whether expression of human FMRP isoforms can also attenuate memory deficiency.

In summary, this study demonstrates that expression of different human FMRP isoforms driven by the human *FMR1* promoter can rectify anxiety-like and ASD-like behaviors and dendritic spine dysmorphologies in *Fmr1*$^{-/y}$ mice without causing any deleterious effects. These findings, together with previous work, further establish the efficacy of AAV-mediated expression of FMRP as a potential long-lasting therapeutic treatment for FXS.

MATERIALS AND METHODS

Animals

Fmr1 KO mice (in FVB background) were from Jackson Laboratory (Bar Harbor, Maine, strain no. 003025)[29] and crossed with FVB mice (from Xiamen University Laboratory Animal Center) to generate *Fmr1*$^{-/y}$ mice and male WT control mice. C57BL/6J WT mice were from Xiamen University Laboratory Animal Center. Mice subjected to the same treatment were housed five per cage and on a 12-h light-dark cycle, with free access to food and water. All animal procedures were conducted in accordance with the National Institutes of Health Guide for the Care and Use of Laboratory Animals and approved by the Animal Ethics Committee of Xiamen University.

Cell culture and transfection

HEK293T cells and SH-SY5Y cells were cultured in Dulbecco's modified Eagle medium supplemented with 10% fetal bovine serum and maintained at 37°C in an incubator containing 5% CO_2. Plasmid transfection was carried out using Turbofect (Thermo Fisher Scientific), following the manufacturer's protocol. Primary neurons, astrocytes, and microglia were derived from neonatal WT mice as described previously.[30]

FMRP isoform 15 transcript generation

Total RNAs were extracted from HEK293T cells and SH-SY5Y cells using the TRIzol reagent (Thermo Fisher Scientific) and transcribed into cDNAs using the ReverTra Ace qPCR RT Kit (Toyobo). PCR was carried out using the primer pair below to amplify full-length FMRP cDNAs. Amplified PCR products were subjected to Sanger sequencing directly and identified as FMRP isoform 15.

FMR1-F: 5′-ATGGAGGAGCTGGTGGTGGAA-3′;

FMR1-R: 5′-TTAGGGTACTCCATTCACGAGTGGTTGC-3′.

Plasmids and AAV packaging

We replaced tdTomato in the pAAV-CAG-tdTomato plasmid (Addgene, no. 59462) with two different human FMR1 transcripts that encode FMRP isoform 1 and FMRP isoform 15, respectively (isoform nomenclature follows that in Pretto et al.[9]). The CAG promoter in pAAV-CAG-tdTomato, pAAV-CAG-FMRP isoform 1, and pAAV-CAG-FMRP isoform 15 plasmids were then replaced with two different *FMR1* endogenous promoter subdomains (P1 and P2) that were synthesized by YouBio (Changsha, Hunan, China) (Figure 1C).

Virus packaging was carried out following a protocol described previously.[31] In brief, pAAV-*FMR1*-P2-tdTomato, pAAV-*FMR1*-P2-FMRP isoform 1, and pAAV-*FMR1*-P2-FMRP isoform 15 plasmids were individually co-transfected with pAAV2/9 (Addgene, no. 112865) and pAd-deltaF6 (Addgene, no. 112867) plasmids into HEK293T cells using PEI. Generated viruses were purified by density gradient centrifugation with iodixanol. Viral titrations were determined using qRT-PCR. Standard curves were generated using plasmids with known copy numbers, and vector genome copies were calculated based on standard curves.

In vivo AAV infection

Packaged AAV2/9s were administered into the brain of P0 mice through bilateral i.c.v. injection following a previously described method.[30] In brief, P0 mice were immobilized via cryo-anesthesia for 3 min. Then 1 μL virus (1.14×10^{12} V.G./mL) was slowly injected into each lateral ventricle (2 mm distance from ventral to skin and 1/3 from the lambda suture to the eye). After each injection, the needle was slowly retracted to prevent backflow. Injected mice were put on a warming pad for body temperature recovery.

Western blotting

Treated cells and brain tissues were lysed in the TNEN lysis buffer (25mM Tris-HCl [pH 7.6], 150 mM NaCl, 1% sodium deoxycholate, 1% NP-40, and 0.1% SDS) supplemented with the protease inhibitor. Equal amounts of protein lysates were subjected to SDS-polyacrylamide gel electrophoresis and proteins were detected by the indicated antibodies. Primary antibodies used were as follows: anti-FMRP (Cell Signaling Technology, 4317S, 1:1,000), anti-NeuN (Cell Signaling Technology, 94403S, 1:1,000), anti-GFAP (Cell Signaling Technology, 3670S, 1:1,000), anti-Iba1 (Wako, 016–20001, 1:1,000), anti-GAPDH (Abways, AB0038, 1:5,000), and anti-α-tubulin (Millipore, MABT205, 1:10,000). HRP-conjugated secondary antibodies used were goat anti-rabbit IgG (H + L), HRP (Thermo Fisher Scientific, 31460, 1:5,000) and goat anti-mouse IgG (H + L), HRP (Thermo Fisher Scientific, 31430, 1:5,000).

Immunofluorescence

Treated mice were anesthetized and intracardially perfused with ice-cold PBS. The brains were dissected quickly and post-fixed in 4% paraformaldehyde at 4°C for 24 h, and cryoprotected in 30% sucrose. Dehydrated tissues were frozen in OCT and cut into 15-μm-thick sections using a freezing microtome (Leica). Mouse coronal slices were blocked in 5% BSA and permeabilized in 0.2% Triton X-100 diluted in PBS at room temperature, and incubated with indicated primary antibodies: anti-FMRP (Cell Signaling Technology, 4317S, 1:50), anti-NeuN (Cell Signaling Technology, 94403S, 1:200), and anti-GFAP (Cell Signaling Technology, 3670S, 1:200) at 4°C overnight. Slices were then stained with fluorescence-conjugated secondary antibody Alexa Fluor 488 goat anti-rabbit IgG (H + L) (Thermo Fisher Scientific, A-11008, 1:400) or Alexa Fluor 594 goat anti-mouse IgG (H + L) (Thermo Fisher Scientific, A-11005, 1:400) for 1 h at room temperature in the dark. Confocal images were captured with the FV1000MPE-B (Olympus) confocal microscope.

Golgi staining

Golgi staining was carried out following the protocol described previously.[32] In brief, mice were anesthetized and brains were collected for Golgi staining using the FD Rapid Golgistain Kit (FD Neuro Technologies) according to the manufacturer's protocol. Images were captured with a laser scanning confocal microscope (Olympus FV1000). Images were calibrated according to the acquisition parameters and spine numbers were counted. Mature and immature spines were defined as described previously[33] with some modifications. The criteria used are as the following: mature: $d_1 \geq 10\ d_2$; immature: $d_1 < 10\ d_2$ and d2 << L, and d1 < d2 (Figure 7A).

Behavioral tests

Treated male mice at age 1.5 months were subjected to behavioral tests. All behavioral experiments were performed and scored by researchers blinded to the genotype. The open-field test, elevated plus maze test, Y-maze test, novel object recognition test, three-chamber social interaction test, nest building test, and self-grooming test were carried out as described previously, and in brief below.[30,32,34,35]

Open-field test

Mice were placed in the center of a square box (40 cm [L] × 40 cm [W] × 40 cm [H]) and allowed to explore freely for 10 min. Time spent in the center and total movement distance were measured by TopScan Lite (CleverSys, Reston, VA).

Elevated plus maze test

The elevated plus maze test consisted of two 30 cm (L) × 6 cm (W) open arms and two 30 cm (L) × 6 cm (W) × 15 cm (H) closed arms. The plus maze is 50 cm high from the ground. Each mouse was placed in the center of the elevated plus maze facing an open arm. Mouse movement was recorded for 5 min. The time spent in open arms and the number of open arm entries were analyzed by TopScan Lite (CleverSys).

Y-maze test

Mice were placed in the center of a Y-shaped maze with three symmetrical arms at 120° (30 cm [L] × 6 cm [W] × 15 cm [H]) from each other and allowed to freely explore the three arms for 5 min. The percentage of spontaneous alternation was calculated automatically by TopScan Lite (CleverSys).

Novel object recognition test

The test consisted of three phases: habituation, training, and test. In the habituation phase, mice were allowed to explore freely an empty arena (40 cm [L] × 40 cm [W] × 40 cm [H]) for 10 min. During the training phase 24 h later, each mouse was individually placed into the arena containing two identical objects that were equidistant from each other, and allowed to explore the objects for 10 min. During the test phase after another 24 h, one object was replaced by an object with a different shape and mice were allowed to explore the novel object and the left familiar object for 10 min. The time spent exploring each object was recorded by TopScan Lite (CleverSys). The time spent exploring the novel object divided by the total exploration time is

defined as the discrimination ratio and was used to measure the recognition memory of each mouse.

Three-chamber social interaction test

This test was carried out in a rectangular, three-chambered box. Each chamber is 40 cm (L) × 22 cm (W) × 23 cm (H). Chamber dividing walls are clear with small openings (5 × 5 cm) as access to each chamber. There is an empty cage in each lateral chamber. The test mouse was first allowed to explore the apparatus for 10 min and then confined in the central chamber. After a strange mouse (S1, age and sex matched to the test mouse) was placed into one of the empty cages, the test mouse was allowed to explore the apparatus for 10 min. Next, another strange mouse (S2, age and sex matched to the test mouse) was placed into the other empty cage, and the test mouse was allowed to explore freely for another 10 min. The movement of the test mouse and its time spent in contact with the cages were recorded by TopScan Lite (CleverSys).

Nest building test

Mice were individually placed in a cage containing a square cotton tissue (3 g) overnight and nest building was scored as following: score 1, cotton tissue rarely touched; score 2, 50%–90% of nesting cotton remains intact; score 3, 50%–90% of nesting cotton was shredded; score 4, more than 90% of nesting cotton was torn and gathered with a flat nest lower than mouse body height; score 5, perfect nest shape.

Self-grooming test

Each mouse was placed individually in a cage (40 cm [L] × 22 cm [W] × 23 cm [H]) with fresh bedding for habituation for 5 min, then mouse spontaneous behaviors were recorded for 10 min to analyze the time spent grooming and the number of bouts.

Statistical analysis

Statistical analysis was performed using the GraphPad Prism 8.0 software (GraphPad Software, La Jolla, CA). All data are presented as the mean ± SEM. Detailed statistical method for each comparison is indicated in figure legends. $p < 0.05$ was considered to be statistically significant.

DATA AVAILABILITY

All data are available in the main text or the supplemental information.

SUPPLEMENTAL INFORMATION

Supplemental information can be found online at https://doi.org/10.1016/j.omtm.2022.10.002.

ACKNOWLEDGMENTS

This work was supported by grants from the National Natural Science Foundation of China (U21A20361, 82130039, U1705285, and 81771377 to Y.-w.Z.; and 92049202 and 92149303 to Hua X.), National Key Research and Development Program of China (2018YFC2000400 to Y.-w.Z.), and The Major Program of Brain Science and Brain-Like Intelligence Technology (2021ZD0202400 to Hua X.).

AUTHOR CONTRIBUTIONS

Y.J., L.H., and Y.-w.Z. designed the research. Y.J., L.H., J.M., Z.W., Y. Zhou, H.Y., and Hui X. conducted the experiments. X.Z., Y. Zhao, J.L., Huaxi X., and C.Z. provided technical and intellectual support. Y.-w.Z. supervised the project. Y.J., L.H., X.Z., and Y.-w.Z. wrote the manuscript. All authors reviewed the manuscript.

DECLARATION OF INTERESTS

The authors declare no competing interests.

REFERENCES

1. Protic, D., Salcedo-Arellano, M.J., Dy, J.B., Potter, L.A., and Hagerman, R.J. (2019). New targeted treatments for fragile X syndrome. Curr. Pediatr. Rev. *15*, 251–258. https://doi.org/10.2174/1573396315666190625110748.
2. Hooper, A.W.M., Wong, H., Niibori, Y., Abdoli, R., Karumuthil-Melethil, S., Qiao, C., Danos, O., Bruder, J.T., and Hampson, D.R. (2021). Gene therapy using an ortholog of human fragile X mental retardation protein partially rescues behavioral abnormalities and EEG activity. Mol. Ther. Methods Clin. Dev. *22*, 196–209. https://doi.org/10.1016/j.omtm.2021.06.013.
3. Shitik, E.M., Velmiskina, A.A., Dolskiy, A.A., and Yudkin, D.V. (2020). Reactivation of FMR1 gene expression is a promising strategy for fragile X syndrome therapy. Gene Ther. *27*, 247–253. https://doi.org/10.1038/s41434-020-0141-0.
4. Sittler, A., Devys, D., Weber, C., and Mandel, J.L. (1996). Alternative splicing of exon 14 determines nuclear or cytoplasmic localisation of fmr1 protein isoforms. Hum. Mol. Genet. *5*, 95–102. https://doi.org/10.1093/hmg/5.1.95.
5. Eichler, E.E., Richards, S., Gibbs, R.A., and Nelson, D.L. (1993). Fine structure of the human FMR1 gene. Hum. Mol. Genet. *2*, 1147–1153. https://doi.org/10.1093/hmg/2.8.1147.
6. Verkerk, A.J., de Graaff, E., De Boulle, K., Eichler, E.E., Konecki, D.S., Reyniers, E., Manca, A., Poustka, A., Willems, P.J., Nelson, D.L., et al. (1993). Alternative splicing in the fragile X gene FMR1. Hum. Mol. Genet. *2*, 1348. https://doi.org/10.1093/hmg/2.8.1348.
7. Brackett, D.M., Qing, F., Amieux, P.S., Sellers, D.L., Horner, P.J., and Morris, D.R. (2013). FMR1 transcript isoforms: association with polyribosomes; regional and developmental expression in mouse brain. PLoS One *8*, e58296. https://doi.org/10.1371/journal.pone.0058296.
8. Khandjian, E.W., Fortin, A., Thibodeau, A., Tremblay, S., Côté, F., Devys, D., Mandel, J.L., and Rousseau, F. (1995). A heterogeneous set of FMR1 proteins is widely distributed in mouse tissues and is modulated in cell culture. Hum. Mol. Genet. *4*, 783–789. https://doi.org/10.1093/hmg/4.5.783.
9. Pretto, D.I., Eid, J.S., Yrigollen, C.M., Tang, H.T., Loomis, E.W., Raske, C., Durbin-Johnson, B., Hagerman, P.J., and Tassone, F. (2015). Differential increases of specific FMR1 mRNA isoforms in premutation carriers. J. Med. Genet. *52*, 42–52. https://doi.org/10.1136/jmedgenet-2014-102593.
10. Dury, A.Y., El Fatimy, R., Tremblay, S., Rose, T.M., Côté, J., De Koninck, P., and Khandjian, E.W. (2013). Nuclear fragile X mental retardation protein is localized to cajal bodies. PLoS Genet. *9*, e1003890. https://doi.org/10.1371/journal.pgen.1003890.
11. Hampson, D.R., Hooper, A.W.M., and Niibori, Y. (2019). The application of adeno-associated viral vector gene therapy to the treatment of fragile X syndrome. Brain Sci. *9*, E32. https://doi.org/10.3390/brainsci9020032.
12. Gholizadeh, S., Arsenault, J., Xuan, I.C.Y., Pacey, L.K., and Hampson, D.R. (2014). Reduced phenotypic severity following adeno-associated virus-mediated Fmr1 gene delivery in fragile X mice. Neuropsychopharmacology *39*, 3100–3111. https://doi.org/10.1038/npp.2014.167.
13. Zeier, Z., Kumar, A., Bodhinathan, K., Feller, J.A., Foster, T.C., and Bloom, D.C. (2009). Fragile X mental retardation protein replacement restores hippocampal

synaptic function in a mouse model of fragile X syndrome. Gene Ther. *16*, 1122–1129. https://doi.org/10.1038/gt.2009.83.

14. Arsenault, J., Gholizadeh, S., Niibori, Y., Pacey, L.K., Halder, S.K., Koxhioni, E., Konno, A., Hirai, H., and Hampson, D.R. (2016). FMRP expression levels in mouse central nervous system neurons determine behavioral phenotype. Hum. Gene Ther. *27*, 982–996. https://doi.org/10.1089/hum.2016.090.

15. Yang, C., Tian, Y., Su, F., Wang, Y., Liu, M., Wang, H., Cui, Y., Yuan, P., Li, X., Li, A., et al. (2022). Restoration of FMRP expression in adult V1 neurons rescues visual deficits in a mouse model of fragile X syndrome. Protein Cell *13*, 203–219. https://doi.org/10.1007/s13238-021-00878-z.

16. Habbas, K., Cakil, O., Zámbó, B., Tabet, R., Riet, F., Dembele, D., Mandel, J.L., Hocquemiller, M., Laufer, R., Piguet, F., and Moine, H. (2022). AAV-delivered diacylglycerol kinase DGKk achieves long-term rescue of fragile X syndrome mouse model. EMBO Mol. Med. *14*, e14649. https://doi.org/10.15252/emmm.202114649.

17. Hirst, M., Grewal, P., Flannery, A., Slatter, R., Maher, E., Barton, D., Fryns, J.P., and Davies, K. (1995). Two new cases of FMR1 deletion associated with mental impairment. Am. J. Hum. Genet. *56*, 67–74.

18. Gholizadeh, S., Halder, S.K., and Hampson, D.R. (2015). Expression of fragile X mental retardation protein in neurons and glia of the developing and adult mouse brain. Brain Res. *1596*, 22–30. https://doi.org/10.1016/j.brainres.2014.11.023.

19. Galvez, R., and Greenough, W.T. (2005). Sequence of abnormal dendritic spine development in primary somatosensory cortex of a mouse model of the fragile X mental retardation syndrome. Am. J. Med. Genet. *135*, 155–160. https://doi.org/10.1002/ajmg.a.30709.

20. McKinney, B.C., Grossman, A.W., Elisseou, N.M., and Greenough, W.T. (2005). Dendritic spine abnormalities in the occipital cortex of C57BL/6 Fmr1 knockout mice. Am. J. Med. Genet. B Neuropsychiatr. Genet. *136B*, 98–102. https://doi.org/10.1002/ajmg.b.30183.

21. Wisniewski, K.E., Segan, S.M., Miezejeski, C.M., Sersen, E.A., and Rudelli, R.D. (1991). The Fra(X) syndrome: neurological, electrophysiological, and neuropathological abnormalities. Am. J. Med. Genet. *38*, 476–480. https://doi.org/10.1002/ajmg.1320380267.

22. Musumeci, S.A., Calabrese, G., Bonaccorso, C.M., D'Antoni, S., Brouwer, J.R., Bakker, C.E., Elia, M., Ferri, R., Nelson, D.L., Oostra, B.A., and Catania, M.V. (2007). Audiogenic seizure susceptibility is reduced in fragile X knockout mice after introduction of FMR1 transgenes. Exp. Neurol. *203*, 233–240. https://doi.org/10.1016/j.expneurol.2006.08.007.

23. Peier, A.M., McIlwain, K.L., Kenneson, A., Warren, S.T., Paylor, R., and Nelson, D.L. (2000). (Over)correction of FMR1 deficiency with YAC transgenics: behavioral and physical features. Hum. Mol. Genet. *9*, 1145–1159. https://doi.org/10.1093/hmg/9.8.1145.

24. Rio, M., Malan, V., Boissel, S., Toutain, A., Royer, G., Gobin, S., Morichon-Delvallez, N., Turleau, C., Bonnefont, J.P., Munnich, A., et al. (2010). Familial interstitial Xq27.3q28 duplication encompassing the FMR1 gene but not the MECP2 gene causes a new syndromic mental retardation condition. Eur. J. Hum. Genet. *18*, 285–290. https://doi.org/10.1038/ejhg.2009.159.

25. Vengoechea, J., Parikh, A.S., Zhang, S., and Tassone, F. (2012). De novo microduplication of the FMR1 gene in a patient with developmental delay, epilepsy and hyperactivity. Eur. J. Hum. Genet. *20*, 1197–1200. https://doi.org/10.1038/ejhg.2012.78.

26. Hickey, S.E., Walters-Sen, L., Mosher, T.M., Pfau, R.B., Pyatt, R., Snyder, P.J., Sotos, J.F., and Prior, T.W. (2013). Duplication of the Xq27.3-q28 region, including the FMR1 gene, in an X-linked hypogonadism, gynecomastia, intellectual disability, short stature, and obesity syndrome. Am. J. Med. Genet. *161A*, 2294–2299. https://doi.org/10.1002/ajmg.a.36034.

27. Hall, S.S., Burns, D.D., Lightbody, A.A., and Reiss, A.L. (2008). Longitudinal changes in intellectual development in children with Fragile X syndrome. J. Abnorm. Child Psychol. *36*, 927–939. https://doi.org/10.1007/s10802-008-9223-y.

28. Kazdoba, T.M., Leach, P.T., Silverman, J.L., and Crawley, J.N. (2014). Modeling fragile X syndrome in the Fmr1 knockout mouse. Intractable Rare Dis. Res. *3*, 118–133. https://doi.org/10.5582/irdr.2014.01024.

29. Consortium, T.D.-B.F.X. (1994). Fmr1 knockout mice: a model to study fragile X mental retardation. Cell *78*, 23–33.

30. Zhang, M., Zhou, Y., Jiang, Y., Lu, Z., Xiao, X., Ning, J., Sun, H., Zhang, X., Luo, H., Can, D., et al. (2021). Profiling of sexually dimorphic genes in neural cells to identify Eif2s3y, whose overexpression causes autism-like behaviors in male mice. Front. Cell Dev. Biol. *9*, 669798. https://doi.org/10.3389/fcell.2021.669798.

31. Challis, R.C., Ravindra Kumar, S., Chan, K.Y., Challis, C., Beadle, K., Jang, M.J., Kim, H.M., Rajendran, P.S., Tompkins, J.D., Shivkumar, K., et al. (2019). Systemic AAV vectors for widespread and targeted gene delivery in rodents. Nat. Protoc. *14*, 379–414. https://doi.org/10.1038/s41596-018-0097-3.

32. Zhao, D., Meng, J., Zhao, Y., Huo, Y., Liu, Y., Zheng, N., Zhang, M., Gao, Y., Chen, Z., Sun, H., et al. (2019). RPS23RG1 is required for synaptic integrity and rescues alzheimer's disease-associated cognitive deficits. Biol. Psychiatry *86*, 171–184. https://doi.org/10.1016/j.biopsych.2018.08.009.

33. Tian, Y., Tang, F.L., Sun, X., Wen, L., Mei, L., Tang, B.S., and Xiong, W.C. (2015). VPS35-deficiency results in an impaired AMPA receptor trafficking and decreased dendritic spine maturation. Mol. Brain *8*, 70. https://doi.org/10.1186/s13041-015-0156-4.

34. Niu, M., Zheng, N., Wang, Z., Gao, Y., Luo, X., Chen, Z., Fu, X., Wang, Y., Wang, T., Liu, M., et al. (2020). RAB39B deficiency impairs learning and memory partially through compromising autophagy. Front. Cell Dev. Biol. *8*, 598622. https://doi.org/10.3389/fcell.2020.598622.

35. Meng, J., Han, L., Zheng, N., Xu, H., Liu, Z., Zhang, X., Luo, H., Can, D., Sun, H., Xu, H., and Zhang, Y.W. (2020). TMEM59 haploinsufficiency ameliorates the pathology and cognitive impairment in the 5xFAD mouse model of alzheimer's disease. Front. Cell Dev. Biol. *8*, 596030. https://doi.org/10.3389/fcell.2020.596030.